

Effect of the surface on the electronic properties of a two-dimensional electron gas as measured by the quantum Hall effect

G. Kopnov,¹ V. Y. Umansky,² H. Cohen,³ D. Shahar,² and R. Naaman¹

¹*Department of Chemical Physics, The Weizmann Institute of Science, Rehovot 76100, Israel*

²*Department of Condensed Matter Physics, The Weizmann Institute of Science, Rehovot 76100, Israel*

³*Department of Chemical Research Support, The Weizmann Institute of Science, Rehovot 76100, Israel*

(Received 4 November 2009; revised manuscript received 22 December 2009; published 20 January 2010)

The effect of the surface treatments on the transport properties of a two-dimensional electron gas was studied at the quantum limit. The surface of the $\text{Al}_{0.36}\text{Ga}_{0.64}\text{As}/\text{GaAs}$ heterostructure was either coated with gold or etched with HCl solution, or etched and then coated by a self-assembled monolayer (SAM) of either phosphonated (ODP- $\text{C}_{18}\text{H}_{39}\text{PO}_3$) or thiolated (ODT- $\text{C}_{18}\text{H}_{37}\text{S}$) molecules. The etching process was found to reduce significantly both the mobility and the charge density. This effect was reversed upon sequential adsorption of the phosphonated SAM. We propose fine tuning of the device performance by the flexible chemistry of the assembled molecules, two of them demonstrated here. The results indicate that the surface oxidation does not necessarily play the dominant role in this respect and, in particular, that octadecane phosphonic acid (ODP) can protect the substrate from both oxidation and the formation of a passivating carbon layer. In contrast, octadecanethiol (ODT) is not stable enough and is not effective in eliminating surface states, as a result devices covered with ODT behave like those with etched surfaces.

DOI: [10.1103/PhysRevB.81.045316](https://doi.org/10.1103/PhysRevB.81.045316)

PACS number(s): 73.43.-f, 68.18.-g, 68.43.-h

I. INTRODUCTION

In submicron devices, a significant portion of the atoms is located at or near the surfaces. Hence, the properties of these surfaces may control, to a large extent, the electronic characteristics of the device. Indeed, it is well established that the surfaces of semiconductor-based devices have to be treated properly in order to eliminate chemical instability that may cause undesired effects. Usually, the surface of semiconductor devices are passivated in order to stabilize their chemical nature and to eliminate reactivity. Si_3N_4 , SiO_2 , and recently Si have often been used for coating GaAs-based devices and for their passivation.¹

Organic self-assembled monolayers (SAM) were shown to be effective as passivation layers. In addition, these monolayers can serve in altering the electronic properties of a substrate. For example, SAMs were shown to affect the critical temperature in ferromagnetic MnGaAs devices² and furthermore, to change the critical current in type II superconductors.³ In addition, new electronic and magnetic properties were discovered when SAM was deposited on various substrates. Novel magnetic properties were observed in diamagnetic gold nanoparticles as well as in gold films covered by thiol-terminated diamagnetic SAM.^{4,5} The magnetic properties were explained by charge transfer between the adsorbed molecules and the gold substrates.^{6,7} It was shown that the observed magnetic effect stems from a collective phenomenon rather than from the individually adsorbed molecules.

In the present work, we investigated the effect of surfaces on the transport properties of two-dimensional electron gas (2DEG) formed near the surface in a GaAs/AlGaAs heterostructure. Specifically we show how two different monolayers consisting of molecules with different binding groups affect the transport properties of the substrate in markedly different ways. The transport measurements in the Quantum

Hall (QH) regime were conducted on devices with five types of surfaces: surfaces as obtained after the device preparation process, surfaces that are coated with gold, etched surfaces, and surfaces coated with SAM, with a thiol or a phosphonate binding group.

QH plateaus, at which the transverse resistivity ρ_{XY} obtains quantized values of $h/\nu e^2$, where ν is an integer, were observed in different types of high mobility, two-dimensional systems. The values of the QH plateaus are independent of the characteristics of individual samples. However, local potential fluctuations in the sample's interior play a major role in the formation of the QH plateaus and in the transition between them.

The Hall resistivity, ρ_{XY} , has quantized values when the longitudinal resistivity, ρ_{XX} , reaches zero. However, in the transition region between adjacent QH plateaus ρ_{XX} increases and goes through a peak. These peaks can be explained by localization/delocalization transitions using the scaling theory of localization.⁸⁻¹⁰ The width of the transition region approaches zero in the limit of zero temperature. However, at finite temperatures (T), the width of the peaks of longitudinal resistance at the transition region acquires a finite width, ΔB , which is predicted to have a power-law dependence $\Delta B \propto T^\kappa$. The existence of the scaling behavior was shown in some experiments to exist in a wide temperature range.¹¹ However, other experiments indicated that the predicted scaling behavior changes with the properties of the samples and in some cases it did not exist.¹²⁻¹⁴ Moreover, it was pointed out that the scaling behavior cannot explain the observed QH to Hall insulator transition.¹⁵ In the present work, we relate to ΔB and use it as an indication of the surface effect on the QH phenomenon.

II. EXPERIMENTAL DETAILS

Hall-bar samples for the magnetotransport measurements were prepared from modulation-doped¹⁶ $\text{Al}_x\text{Ga}_{1-x}\text{As}/\text{GaAs}$

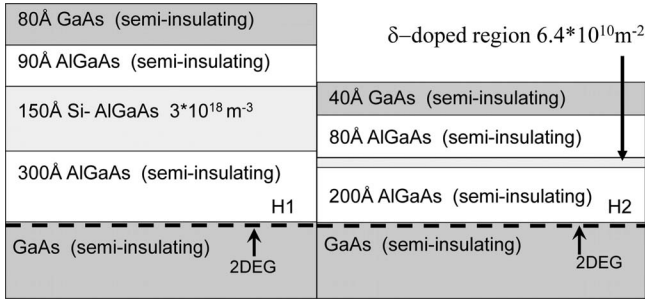


FIG. 1. Description of the schematic layer of the H1 and H2 heterostructures. The H1 heterostructure has a finite-sized Si donor layer with 2DEG 61 nm below the surface. A second heterostructure, termed H2, had a thin δ -Si doping layer when 2DEG was buried at a depth of 32 nm.

heterostructures where $x=0.36$. These heterostructures were grown on a semi-insulating GaAs substrate by a molecular-beam epitaxy technique. Figure 1 shows schematically the layers' structure. High-mobility 2DEG was formed at the interface between the undoped $\text{Al}_x\text{Ga}_{1-x}\text{As}$ spacer and the GaAs layers.¹⁷ Two types of heterostructures were used. The first had the 2DEG layer located 61 nm below the surface and was termed H1 (deep 2DEG). It had a typical electron density and a mobility of $n_s=1.9 \times 10^{11} \text{ cm}^{-2}$ and with $\mu=3 \times 10^5 \text{ cm}^2 \text{ V}^{-1} \text{ s}^{-1}$, respectively, as measured at 260 mK. The second heterostructure is δ doped, where the Si-doping layer was a few atomic layers thick. In this type of heterostructure the 2DEG is formed 32 nm beneath the surface; it was termed H2 (shallow 2DEG). The typical electron density and mobility are $3 \times 10^{11} \text{ cm}^{-2}$ and $\mu=5 \times 10^4 \text{ cm}^2 \text{ V}^{-1} \text{ s}^{-1}$, respectively, as measured at 260 mK.

The devices for the magnetotransport measurements consisted of two queued Hall-bar samples each $275 \mu\text{m}$ long [Fig. 2(A)]. The samples were prepared by standard lithographic and etching techniques.¹⁸ Ohmic contacts to the 2DEG were made from five metallic layers of Ni/Ge/Au/Ni/Au, which were successively deposited on the heterostruc-

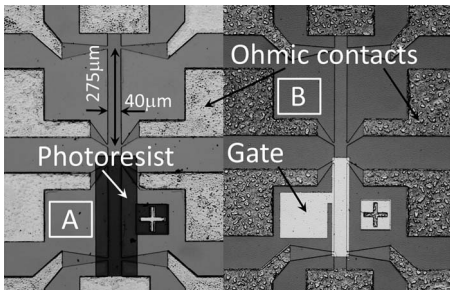


FIG. 2. Images acquired by the optical microscope of the sample (a) for the chemical modification and another sample (b) with a metallic top gate. The sample has a $700\text{-}\mu\text{m}$ -long and $40\text{-}\mu\text{m}$ -wide 2DEG strip between the two current leads. An additional eight potential leads divide the long strip into two queued Hall-bar devices. The molecules were adsorbed on the photoresist-free device of the 2DEG strip after native oxide was removed from it. The photoresist protected the second device of the 2DEG channel surface from the acid. This part of the sample served as a reference for the magnetotransport measurements.

ture in the custom-made e-beam evaporation system. After the lift-off procedure, the metal layers were alloyed with the heterostructure at $460 \text{ }^\circ\text{C}$ in H/Ar (5:95) atmosphere.¹⁹

The magnetotransport measurements were performed at low temperatures in top-loading ^3He or dilution refrigerators equipped with 8 and 12 T superconducting magnets, respectively (Oxford instruments). The magnetic field was applied perpendicular to the plane of the 2DEG. In all measurements, the magnetic field was swept at a constant rate and in the same direction. In order to avoid electron heating, we used an alternating current of 10 nA or less at a frequency of 14 Hz. The transverse potential difference (V_{XY}), which was measured perpendicular to the current, and the longitudinal (V_{XX}) potential difference, which was measured parallel to the current, were amplified by two low-noise differential preamplifiers. Each amplifier had a gain of 10^3 . The amplified signals were measured by two lock-in amplifiers (EG and G 7265).

The electron density, n_s , was extracted from the low magnetic field measurements, where the Hall resistance was not quantized, and from the Shubnikov de Haas (SdH) oscillation peaks measured in the longitudinal resistance.²¹ The electron density was extracted from the measured Hall potential by the relation $n_s=I/e(\partial V_{XY}/\partial B)$, where I is the current that flows through the 2DEG channel, e is the electron's charge, and B is the external magnetic field. The electron density was also calculated from the expression $n_s=2e/h(1/B_1-1/B_2)$, where B_1 and B_2 are the magnetic fields corresponding to two successive peaks in the measured SdH oscillations. The electron mobility was extracted from the relation $\mu_0=LI/n_s e W V_{XX}^0$, where L is the distance between the potential contacts in the direction parallel to I , W is the width of the channel, and V_{XX}^0 is the longitudinal potential difference, measured at zero magnetic field.

In the first part of the experiments, the sample with a metallic top gate was prepared from the H1 heterostructure and was termed H1a. The metallic gate was evaporated on top of the 2DEG channel covering only half of it whereas the second part of the sample was left uncovered [Fig. 2(B)]. The gate consisted of a Ti adhesion layer 20 nm thick, on top of which a layer of 100 nm of Au was deposited. The Schottky top gate²⁰ was used to determine the electron-scattering mechanism and to compare between the electronically driven gate operation²¹ and the molecularly induced effects. Electrical potential, V_G , was applied between the electrical ground and the top gate at 260 mK. The gate potentials $|V_G| \leq 100 \text{ mV}$ were chosen to be within the linear dependence of electron density on V_G .

In the second part of the experiments, the surface of the heterostructure was chemically modified. Samples that were prepared from H1 and H2 heterostructures are referred to H1b and H2b, respectively. Each device was divided into two parts: one part of the sample was protected by positive photoresist (Shipley 1813) whereas the second part was left uncovered. The uncovered surface was then chemically processed by removing the oxide layer by dipping the sample into the HCl:H₂O (1:1) solution for 30 s, then rinsing it with distilled (18 M Ω) water and drying it afterward with N₂ gas.²² After the etching, the protective photoresist layer was removed. In order to dissolve the photoresist layer, the

TABLE I. Surface element analysis performed by XPS of the chemically treated GaAs samples. After the etching, the oxygen content was reduced and the amount of carbon increased, compared with the as cut sample. The etched and sequentially covered by SAM sample had a lower amount of GaAs oxide and an excess of oxygen. Additionally, the total carbon content observed with the monolayer corresponds to the amount of carbon in the molecular layer. The oxygen that is not associated with the GaAs oxide or carbon oxide was called excess.

| Sample\compound | GaAsO _x (Å) | C and O (Å) | O excess content (%) |
|--|---------------------------|----------------|-------------------------|
| As cut | 13.4 | 10.6 | 11 |
| Etched | 11.4 | 14 | 7 |
| Etched+C ₁₈ H ₃₉ PO ₃ | 8.3 | * | 4.5 |

samples were immersed either in a clean solvent, dry tetrahydrofuran (THF) or dry toluene, for 10 s and then dried with N₂.

The third part of the experiment included the oxide-removal procedure described previously. In addition, immediately after the protective photoresist layer was washed, the samples were dipped in a solution of amphiphilic molecules for 12 h. The solution consisted of octadecane-phosphonic (ODP) acid (C₁₈H₃₉PO₃) (Polycarbon Industries) dissolved in dry THF (Refs. 2 and 23) or of octadecane-thiol (C₁₈H₃₇S-ODT) molecules dissolved in anhydrous toluene. Then the samples were washed in clean solvent and mounted on the sample holder in order to measure the magnetotransport. The samples that were prepared from the H1 heterostructure were termed H1c and those from the H2 heterostructure were termed H2c.

The quality of the monolayer and the chemical composition of the etched GaAs surface was examined by x-ray photoelectron spectroscopy (XPS) using the Kratos AXIS-HS system at a source power of 75 W and detection pass energies ranging between 20 and 80 eV. Stability under the x-ray beam was confirmed by performing repetitive scans on fixed spots. The inelastic mean-free path of the ejected electrons, λ was assumed to be 33 Å for the organic material and 25 Å for the inorganic one. The thickness of the layer, d , was calculated from the relation $d = \lambda \ln(1 + R)$, where $R = I_{SUB}/I_{LAY}$.²⁴ I_{SUB} and I_{LAY} are the (total) measured intensities from the substrate and from the top layer, respectively.

III. RESULTS

The surfaces of the devices were modified so that five types of devices were investigated: as made, etched, followed by adsorption of two types of SAM, and a device coated with gold. For chemical characterization, each type was XPS studied. The results are presented in Table I, showing that both in the case of an untreated sample or a sample covered with the SAM, the GaAs surface is covered with an immediate layer of oxide. However, in the case of the etched sample, the surface is covered with unoxidized carbon. Notably, the amount of carbon content after the ODP SAM adsorption nicely matches the expected carbon quantity in the

organic SAM. Hence, the adsorption of the ODP SAM results in an essentially complete replacement of the contaminating unoxidized carbon.

The integer quantum-Hall effect (IQHE) was observed in all devices.²⁵ Electron density and mobility were extracted from the ρ_{XY} and $\rho_{XX} = V_{XX}W/IL$ measured values at a constant temperature of 260 mK. The “as prepared” (asp) and the modified devices were situated in proximity to each other. As a result, variation between the two devices in the electron mobility and electron density owing to the nonhomogeneity was minimal. This consistency was verified by several measurements. In addition, it was verified that the protective photoresist coating on top of the 2DEG channel did not produce significant changes in the magnetotransport properties. Therefore, all the changes observed in the chemically modified surfaces must result from the chemical process.

Figure 3 shows measurements acquired from the samples where the 2DEG is located 62 nm below the surface. The ρ_{XX} and ρ_{XY} traces were measured at 260 mK in three different samples. The H1a sample was covered by a metallic gate; H1b was etched, and the H1c sample was etched and covered by ODP SAM. Each plot contains two sets of ρ_{XX} and ρ_{XY} traces: one set is obtained from devices with untreated (as prepared—asp) surfaces, namely, with no coating, and the second set is obtained from devices with modified surfaces.

The measured electron densities extracted from the Hall resistances and from the SdH oscillations had similar values within 3% in all measured devices. Figure 3(A) shows results obtained by measuring the H1a sample when the gate was electrically grounded. The electron density of the asp device of the H1a sample was $2.5 \times 10^{15} \text{ m}^{-2}$ and that of the sample with the metallic gate was $2 \times 10^{15} \text{ m}^{-2}$. The electron mobility decreased from 72 $\text{m}^2/\text{V s}$ in the asp device to 16 $\text{m}^2/\text{V s}$ in the devices covered with the metallic gate. On the other hand, the amplitude of the SdH oscillations in ρ_{XX} increased after the surface was covered by the metal. Furthermore, after the metal was deposited, the half width of the peak in ρ_{XX} , $\Delta B_{1/2}$, at the transition between the filling factors 1 and 2, increased from 0.31 to 0.74 T. $\Delta B_{1/2}$ of the peak in ρ_{XX} is defined as the distance between the two extreme values in $\partial\rho_{XX}/\partial B$.¹¹

Figure 3(B) presents the magnetotransport measurements for the H1b device. The electron mobility was reduced from the 33 $\text{m}^2/\text{V s}$, as found in the asp device, to 16 $\text{m}^2/\text{V s}$ for the etched devices. The measured electron densities in both devices did not change upon etching and were $2 \times 10^{15} \text{ m}^{-2}$. However, the amplitude of the SdH oscillations increased after the etching procedure. In addition, $\Delta B_{1/2}$ at the $\nu: 1 \rightarrow 2$ transition increased from 0.34 to 0.6 T after the etching.

Figure 3(C) displays the results obtained with the H1c sample. The measured electron densities in both devices were the same $2.1 \times 10^{15} \text{ m}^{-2}$ whereas the electron mobility decreased slightly from 38 $\text{m}^2/\text{V s}$ in the asp device to 35 $\text{m}^2/\text{V s}$ in the device that was etched and covered with the ODP monolayer.

Additionally, measurements of the gated device in the H1a sample were performed with different gate potentials. The measured electron density was linearly dependent on the

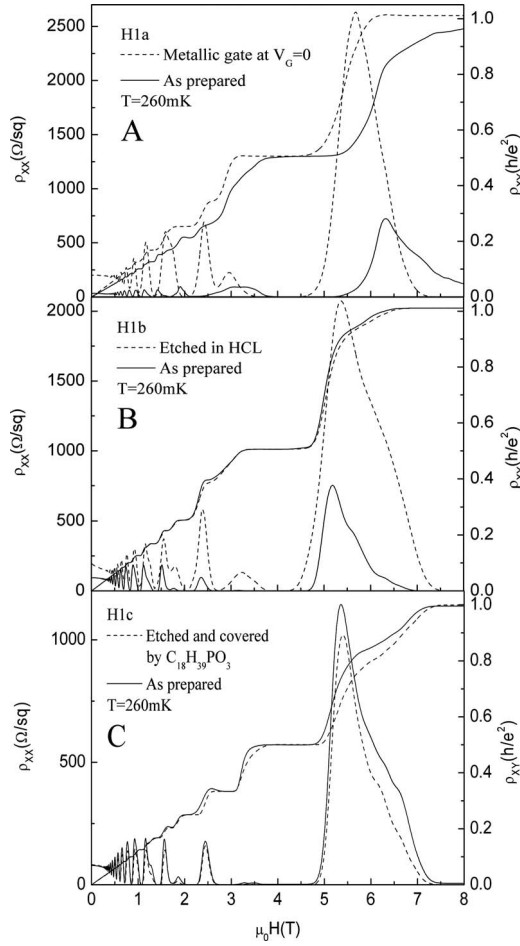


FIG. 3. Magnetoresistance (ρ_{XX}) and Hall (ρ_{XY}) resistances measured versus an externally applied magnetic field showing IQHE. Measurements of the H1a sample at $V_G=0$ are shown in plot A. The dashed line corresponds to part of the 2DEG channel that was covered by the metal gate, and the solid line denotes the asp part of the same sample. Plot B represents the H1b sample measurements. The etched part of the sample is represented by the dashed line and the asp part is represented by the solid line. Sample H1c, which was etched and covered by molecules, is shown in plot C. The solid line denotes the asp part and the dashed one denotes the part of the sample modified with molecules.

applied voltage. On the other hand, the electron mobility showed a power-law dependence versus the electron density, $\mu \propto n_s^\gamma$, where $\gamma \approx 1.5$ is the fitting parameter (see Fig. 4).

Figure 5 shows magnetotransport measurements of the samples prepared from the heterostructure with 2DEG located 32 nm below the surface. The results from the etched and the asp devices (assigned as H2b) are shown in Fig. 5(A). In this case, the electron density was reduced from $2.9 \times 10^{15} \text{ m}^{-2}$ for the asp device down to $1.9 \times 10^{15} \text{ m}^{-2}$ in the etched device. The electron density in the asp device measured from SdH oscillations was similar within 3% of the value measured from ρ_{XY} . On the other hand, in the etched device the electron density extracted from the SdH oscillations was 8% higher than that calculated from the slope of the ρ_{XY} . In addition, the etched device showed a lower electron mobility of $1.2 \text{ m}^2/\text{V s}$ compared with that of the asp device, which was found to be $5.5 \text{ m}^2/\text{V s}$. The am-

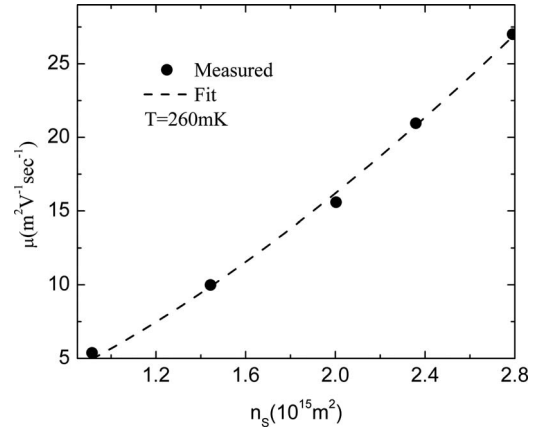


FIG. 4. The plot shows the measured electron mobility vs the measured electron density of the H1a sample. The fitted (dashed) curve had a power-law dependence where $\mu \propto n_s^{1.5}$.

plitude of the SdH oscillations increased in the etched device compared with the asp one. However, $\Delta B_{1/2}$ of the ρ_{XX} peak at the $\nu:1 \rightarrow 2$ transition decreased in the etched device to 0.36 from 0.52 T in the asp device.

Figure 5(B) presents the measurements acquired from sample H2c, which was etched and covered by ODP SAM. The electron mobility decreased from $6.9 \text{ m}^2/\text{V s}$ in the asp device to $4 \text{ m}^2/\text{V s}$ in the device that was etched and cov-

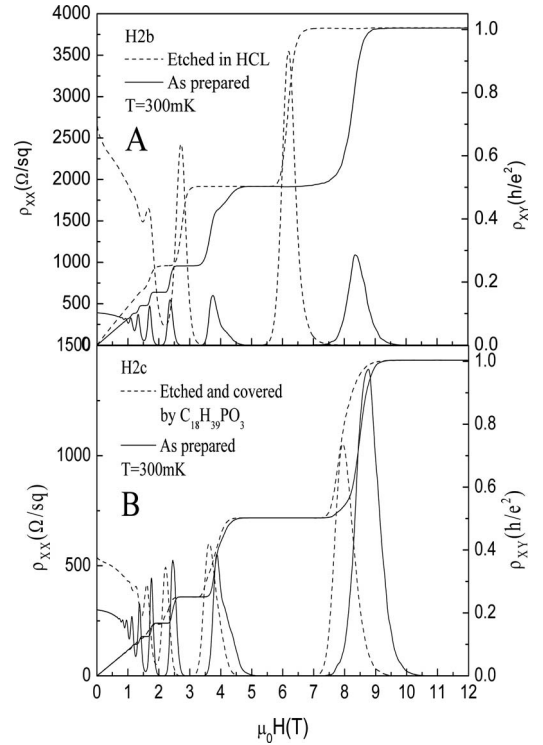


FIG. 5. Magnetoresistance (ρ_{XX}) and Hall (ρ_{XY}) resistances measured versus an externally applied magnetic field. Plot (a) shows measurements of the H2b sample. As prepared, part of the sample is represented by a solid line and the etched one is represented by a dashed line. At plot (b) the curves belong to the sample H2c. The etched and molecules covered by part of the sample are described by the dashed curve whereas the solid curve belongs to the prepared part of the same sample.

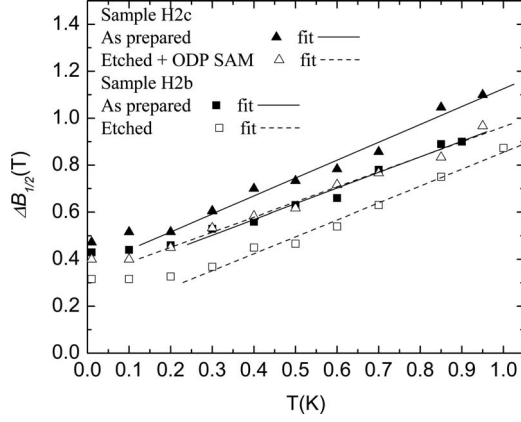


FIG. 6. The measured $\Delta B_{1/2}$ of the ρ_{XX} peaks at the $\nu:1 \rightarrow 2$ transition versus the temperature. Sample H2c, which was etched and covered by molecules, is represented by triangles. Full triangles relate to the asp device whereas the empty ones represent the results from the modified device. The lines represent linear fit to the measured data, where the solid line is the fit to the asp sample and dashed line stands for the modified device. The H2b only etched sample is represented by squares. The full squares stand for measurements done on the asp device and the empty ones designate the etched device in the same sample.

ered by ODP SAM. On the other hand, the electron densities measured in both devices, based on the ρ_{XY} slopes, were identical, $3 \times 10^{15} \text{ m}^{-2}$. The electron density measured by the SdH oscillations in the asp device differed by 3% only from the density measured by the Hall effect. However, the electron density obtained from the SdH oscillations for the monolayer-coated device was 8% higher than that found from the ρ_{XY} slope.

In order to verify the robustness of the surface chemical modifications, several etched devices were measured after being stored in a clean solvent for a few days. The etching effect on the transport properties was clearly observable even after several days.

Samples H2b and H2c were measured at temperatures (T) ranging between 0.01 and 1 K. The $\Delta B_{1/2}$ of the ρ_{XX} peaks in the $\nu:1 \rightarrow 2$ transition were extracted from these measurements, as shown in Fig. 6. In all four devices the value of the $\Delta B_{1/2}$ saturates below 0.2 K. Above 0.2 K, the best fit to the measured data was achieved by the first-order polynomial $\alpha + \beta \cdot t$. In the case of the H2b sample, the coefficients found were $\alpha=0.32$, $\beta=0.64$ and $\alpha=0.16$, $\beta=0.68$ for the asp and

for the etched devices, respectively. In the sample H2c the fitted coefficients were $\alpha=0.32$, $\beta=0.71$ and $\alpha=0.31$, $\beta=0.64$ for the asp device and for the device etched and covered by ODP SAM, respectively. The fitted values of β coefficient vary by 10% only from device to device, independent of the surface treatment. However, the fitted α value in the etched device is only half of that found in the other devices.

Several samples with 2DEG located 62 and 32 nm below the surface were etched and covered with octadecanethiol (ODT) SAM. The adsorption of the ODT SAM did not affect the magnetotransport properties and they were similar to those of the only etched surface. Table II summarizes the results obtained with the various samples.

IV. DISCUSSION

The goal of the present work was to probe the effect of the surface on the electronic properties of a 2DEG located a few tens of nanometers below this surface. Specifically we demonstrated variations in the surface effect achieved with different self-assembled monolayers, ODP and ODT. The resulting changes in the surface's electronic structure were monitored by the magnetotransport properties of modulation-doped field-effect transistor structures. These structures were chosen because their transport properties are highly sensitive to any change in the electronic potential, due to their high electron density and high electron mobility.

Five types of structures were probed: bare surface (as prepared), devices covered with a metal gate, etched, and coated with self-assembled monolayers bound to the substrate either by a thiol or by phosphonate groups. In the following discussion all the results will be discussed relative to the as prepared device.

The metal-covered device showed decreased electron density and mobility owing to the formation of depletion region below the surface. When contact is created between the p -type semiconductor and the metal, which has a lower work function than the semiconductor, a Schottky barrier is formed. As a result, negative charge is accumulated at the semiconductor side of the contact. The source of the negative charge in the heterostructure is most likely the doping layer. Therefore, the increased number of electrons transferred to the surface should lower the electron density in the 2DEG. A decrease in the electron mobility can therefore result from

TABLE II. The samples measured and the measured parameters.

| Sample | As prepared (asp) | | | Observed relative shift from the asp sample after surface treatment | | |
|--------|-------------------------------------|--------------------------------------|-------------------------|---|---|-------------------------|
| | n (10^{15} m^{-2}) | μ ($\text{m}^2/\text{V s}$) | $\Delta B_{1/2}$ (T) | Δn (10^{15} m^{-2}) | $\Delta \mu$ ($\text{m}^2/\text{V s}$) | $\Delta B_{1/2}$ (T) |
| H1a | 2.5 | 72 | 0.31 (0.26 K) | -0.5 | -56 | +0.43 |
| H1b | 2 | 33 | 0.34 (0.26 K) | 0 | -17 | +0.26 |
| H1c | 2.1 | 38 | 0.34 (0.26 K) | 0 | -3 | +0.04 |
| H2b | 2.9 | 5.5 | 0.52 (0.3 K) | -1 | -4.3 | -0.16 |
| H2c | 3 | 6.9 | 0.6 (0.3 K) | 0 | -2.9 | -0.07 |

the increased amount of ionized impurities that lose “their” electrons in compensating for the electrostatic charge near the surface. Ionized impurities are known to be the major source of electron scattering in this type of heterostructures.^{26,27} This can indeed be verified by the relation found between the mobility and charge density, $\mu \propto n_s^\gamma$, $\gamma \approx 1.5$ when these properties were measured as a function of the gate voltage.

The etching of the surface of the 2DEG channel leads to a drop in the electron mobility in all devices. However, with the shallow 2DEG, located 32 nm under the surface, not only the mobility changes, but the electron density decreases as well. The close resemblance of the observed changes in the magnetotransport properties for the metal-coated device and the etched surface leads to the conclusion that in both cases the changes have the same origin. Namely, the etching procedure leads to the creation of new surface states.²⁸

There are two reasons for greater response in devices prepared from the heterostructure with a shallow 2DEG layer. First, the doping layer was situated closer to the surface than in those heterostructures with a deep 2DEG layer. Second, the thickness of the donor layer is atomically thin in the shallower case, which is a delta-doped heterostructure, compared with the other type of heterostructure with a doping layer thickness of many nanometers. Therefore, the shallower 2DEG is more sensitive to changes in the surface’s electronic structure.

When the etched surface was covered by the ODP SAM, the electron mobility increased in all devices. Moreover, in the case of the 32-nm-deep 2DEG, the electron density increased after the adsorption of the ODP SAM. This finding suggests that the molecules with phosphonic acid linkers, adsorbed on the etched GaAs surface, eliminated the surface states, namely, the depletion layer formed by etching. On the other hand, SAM adsorption via thiol linkers on the etched surface did not change the magnetotransport properties at all. The major reason for this interesting observation lies in the molecule-substrate bond type. The phosphonic acid binds to the GaAs surface via a strong P-O-Ga bond whereas the thiols are attached to the As sites²³ in a much weaker and unstable bond.

The XPS measurements indicate that the nature of the adsorber is correlated with the measured transport properties. Upon ODP adsorption, the surface was not oxidized and did not attract further carbon adsorption (see Table I). This is in contrast to the case of ODT monolayer, that allows the growth of both surface oxides and carbon contamination on the GaAs surface.²⁹ In fact, the transport properties are found to better correlate with the formation of the carbon layer rather than with the oxide layer. Namely, the mobility is lower when the surface is covered with directly adsorbed carbon.

The etching process did affect the temperature-dependent measurements of the localization/delocalization transition where $\nu:1 \rightarrow 2$ whereas sequential adsorption of the ODP SAM on the etched surface eliminated this effect. The observed decrease in electron mobility in correlation with the changes in the localization/delocalization transition suggests

that these phenomena are related. The increased amount of ionized impurities that increased the electron-scattering rate could alter the QH-metal transition as well. It was shown experimentally that lowering the electron mobility by implanting acceptors or donors at the vicinity of the GaAs/AlGaAs interface altered the scaling behavior of the localization/delocalization transition.^{12,30} The change in the scaling behavior was attributed to strong electron scattering by the implanted charged impurities. Hence, again there is an indication that the etching causes mainly variations in mobility, similar to the effect of implanting charge impurities.

V. CONCLUSIONS

Applying magnetotransport measurements to the surface at subkelvin temperatures, we found that charge redistribution was induced by different chemical treatments of the GaAs surface. As a result, a large decrease in the electron mobility was measured after the 2DEG surface channel was etched. For a shallow 2DEG layer, the etching induced also a moderate reduction in electron density; however, after the etched 2DEG channel’s surface was covered by ODP SAM, the measured electron density was identical to the values obtained prior to etching. Moreover, the measured electron mobility was identical or very close to the values measured prior to etching. Remarkably, devices covered with ODT exhibit the same properties as devices with etched surfaces. When many surface states exist, e.g., after etching, the depletion layer formed reduces the charge mobility. Carbon layer that is formed on top of the surface “protects” the surface states and does not allow their annihilation by reaction. The ODP strongly reacts with the critical surface states and hence reduces their number, thereby causing a significant increase in the device charge mobility.

Temperature-dependent measurements of the conductivity peak in the transition region between filling factors 1 and 2 in the quantum-Hall effect did not show a scaling behavior. The measured half width of the conductivity peak was linearly dependent on temperature. However, it was found that the half width of the peak, at the limit of zero temperature, decreased after the surface of the 2DEG channel was etched. On the other hand, the measured half width, when the surface was etched and covered by ODP SAM, became identical to the one measured before etching.

In conclusion, it was shown that changes in the local electronic structure of the GaAs surface formed by carbon adsorbates upon etching in an HCl water solution were abrogated by the successive adsorption of the ODP SAM. This effect did not take place upon adsorption of ODT. Self-assembly of molecular layers is further proposed as a flexible means for finely modifying device properties.

ACKNOWLEDGMENTS

The authors would like to thank Y. Gross for his help with the rapid thermal process and M. Ovadia for his help with the transport measurements setup. R.N. and G.K. acknowledge the partial support of the Israel Science Foundation and the Schmidt Minerva Center.

- ¹H. Hasegawa and M. Akazawa, *Appl. Surf. Sci.* **255**, 628 (2008).
- ²T. C. Kreutz, E. G. Gwinn, R. Artzi, R. Naaman, H. Pizem, and C. N. Sukenik, *Appl. Phys. Lett.* **83**, 4211 (2003); I. Carmeli, F. Bloom, E. G. Gwinn, T. C. Kreutz, C. Scoby, A. C. Gossard, S. G. Ray, and R. Naaman, *ibid.* **89**, 112508 (2006).
- ³Dm. Shvarts, M. Hazani, B. Ya. Shapiro, G. Leituss, V. Sidorov, and R. Naaman, *Europhys. Lett.* **72**, 465 (2005).
- ⁴P. Crespo, R. Litrán, T. C. Rojas, M. Multigner, J. M. de la Fuente, J. C. Sánchez-López, M. A. García, A. Hernando, S. Penadés, and A. Fernández, *Phys. Rev. Lett.* **93**, 087204 (2004).
- ⁵I. Carmeli, V. Skakalova, R. Naaman, and Z. Vager, *Angew. Chem., Int. Ed.* **41**, 761 (2002).
- ⁶A. Hernando, P. Crespo, and M. A. Garcia, *Phys. Rev. Lett.* **96**, 057206 (2006).
- ⁷Z. Vager and R. Naaman, *Phys. Rev. Lett.* **92**, 087205 (2004).
- ⁸H. P. Wei, D. C. Tsui, and A. M. M. Pruisken, *Phys. Rev. B* **33**, 1488 (1986).
- ⁹A. M. M. Pruisken, *Phys. Rev. Lett.* **61**, 1297 (1988).
- ¹⁰B. Huckestein and B. Kramer, *Phys. Rev. Lett.* **64**, 1437 (1990).
- ¹¹H. P. Wei, D. C. Tsui, M. A. Paalanen, and A. M. M. Pruisken, *Phys. Rev. Lett.* **61**, 1294 (1988).
- ¹²S. Koch, R. J. Haug, K. v. Klitzing, and K. Ploog, *Phys. Rev. B* **43**, 6828 (1991).
- ¹³A. A. Shashkin, V. T. Dolgoplov, and G. V. Kravchenko, *Phys. Rev. B* **49**, 14486 (1994).
- ¹⁴N. Q. Balaban, U. Meirav, and I. Bar-Joseph, *Phys. Rev. Lett.* **81**, 4967 (1998).
- ¹⁵D. Shahar, M. Hilke, C. C. Li, D. C. Tsui, S. L. Sondhi, J. E. Cunningham, and M. Razeghi, *Solid State Commun.* **107**, 19 (1998).
- ¹⁶V. Umansky, R. de-Picciotto, and M. Heiblum, *Appl. Phys. Lett.* **71**, 683 (1997).
- ¹⁷R. Dingle, H. L. Stormer, A. C. Gossard, and W. Wiegmann, *Appl. Phys. Lett.* **33**, 665 (1978).
- ¹⁸R. E. Williams, *Modern GaAs Processing Methods* (Artech House, London, UK, 1990), p. 95–136.
- ¹⁹D. Jucknischke, H. Buhlmann, R. Houdr, M. Ilegems, M. A. Py, B. Jeckelmann, and W. Schwitz, *IEEE Trans. Instrum. Meas.* **40**, 228 (1991).
- ²⁰A. Kurobe, J. E. F. Frost, M. P. Grimshaw, D. A. Ritchie, G. A. C. Jones, and M. Pepper, *Appl. Phys. Lett.* **62**, 2522 (1993).
- ²¹J. H. Davies, *The Physics of Low-Dimensional Semiconductors* (Cambridge University Press, Cambridge, England, 1998).
- ²²M. Lebedev, E. Mankel, T. Mayer, and W. Jaegermann, *J. Phys. Chem. C* **112**, 18510 (2008).
- ²³A. M. Botelho do Rego, A. M. Ferraria, J. El Beghdadi, F. Debontridder, P. Brogueira, R. Naaman, and M. Rei Vilar, *Langmuir* **21**, 8765 (2005).
- ²⁴D. Briggs and M. P. Seah, *Practical Surface Analysis*, 2nd ed. (Wiley, New York, 1990), Vol. 1.
- ²⁵K. v. Klitzing, G. Dorda, and M. Pepper, *Phys. Rev. Lett.* **45**, 494 (1980).
- ²⁶D. C. Tsui, A. C. Gossard, G. Kaminsky, and W. Weignann, *Appl. Phys. Lett.* **39**, 712 (1981).
- ²⁷T. J. Ando, *J. Phys. Soc. Jpn.* **51**, 3900 (1982).
- ²⁸L. Kronik and Y. Shapira, *Surf. Sci. Rep.* **37**, 1 (1999).
- ²⁹T. Aqua, H. Cohen, A. Vilan, and R. Naaman, *J. Phys. Chem. C* **111**, 16313 (2007).
- ³⁰R. J. Haug, R. R. Gerhardts, K. v. Klitzing, and K. Ploog, *Phys. Rev. Lett.* **59**, 1349 (1987).